

## Experimental confirmation of nonequilibrium steady-state theory: Brillouin scattering in a temperature gradient

H. Kiefte, M. J. Clouter, and R. Penney

*Department of Physics, Memorial University of Newfoundland, St. John's,  
Newfoundland A1B 3X7 Canada*

(Received 29 May 1984)

The present results confirm the existence of the Brillouin intensity asymmetry induced by a thermal gradient both in a liquid (water) and, for the first time, in a solid (fused quartz). This provides a direct check of the statistical methods used in nonequilibrium physics. For water, the data show excellent agreement with linear theory. Finite size effects are clearly evident and it is suggested that wall effects are more important than mode-coupling nonlinearities.

Presently there is a great deal of interest in fluids out of equilibrium.<sup>1</sup> A number of recent theoretical predictions have been worked out and reviewed by Tremblay<sup>2</sup> (see also Ref. 3) for fluids in nonequilibrium steady state, particularly the problem of Brillouin scattering in a simple liquid subjected to a temperature gradient.

The early history of this work involved light scattering in a nonuniformly heated solid and has been summarized by Fabelinskii.<sup>4</sup> The only other relevant discussion for the case of solids was by Griffin<sup>5</sup> in 1968. Most recently, the theoretical problem of Brillouin scattering in a fluid subjected to a temperature gradient has been solved by several independent groups: Procaccia, Ronis, and Oppenheim<sup>6,7</sup> using nonlinear response theory, Kirkpatrick, Cohen, and Dorfman<sup>8,9</sup> using kinetic theory, and others<sup>3,10-14</sup> such as Tremblay using fluctuating hydrodynamics.

The same general result is obtained, when a fluid is brought out of equilibrium by a steady temperature gradient, an asymmetry in the intensities of the two Brillouin peaks results. Qualitatively the effect arises because, for  $\vec{q}$  along  $\vec{\nabla} T$ , there are more sound waves with wave vector  $-\vec{q}$  absorbed than sound waves with wave vector  $+\vec{q}$  emitted<sup>2,3</sup> or, more generally, because there exist long-range correlations in the fluctuations of dissipative states. Ignoring the effect of the boundary of the fluid, the non-plane-wave character of the light source, and mode-coupling nonlinearities the Brillouin asymmetry  $\epsilon$  is given, by the above theories, to be

$$\epsilon = \frac{v}{2\Gamma T} \frac{\hat{q} \cdot \vec{\nabla} T}{q^2}, \quad (1)$$

where

$$\epsilon = [I(-\nu_s) - I(+\nu_s)] / [I(-\nu_s) + I(+\nu_s)],$$

and  $I(+\nu_s)$  and  $I(-\nu_s)$  are the integrated intensities of the upshifted and downshifted Brillouin components, respectively;  $\nu$  is the sound velocity,  $q$  the acoustic or scattering wave vector,  $\Gamma$  is the sound attenuation coefficient such that  $\Gamma q^2$  is the half-width at midheight of a Brillouin line,  $T$  is the temperature, and  $\vec{\nabla} T$  the temperature gradient. Boundary effects have been investigated in detail by Satten and Ronis<sup>14</sup> and nonlinear effects in  $\vec{\nabla} T$  (and boundary effects, although less extensively) by Kirkpatrick, Cohen, and Dorfman.<sup>9</sup>

It is important to verify these predictions experimentally as a test of the methods used in nonequilibrium physics.

Since the asymmetry has both a  $1/q^2$  and  $\nabla T$  dependence, the Brillouin experiments must be performed at very low scattering angles ( $\sim 1^\circ$ ) and with high-temperature gradients. These conditions make the experiments inherently difficult. Such experiments have previously been carried out with water by Beysens, Garrabos, and Zalczer,<sup>15</sup> but unfortunately, for conditions under which the mean free path of the sound waves was larger than the cell dimensions. The Brillouin intensity asymmetry was observed but with a linear variation about three times weaker than predicted by Eq. (1).

In the present work, these experiments were initially attempted with liquid oxygen because of the advantages offered by low  $T$ , small  $\Gamma$ , and large liquid range. The asymmetry effect did appear to be there; however, no firm measurements were made due to quick onset of Rayleigh-Bénard instability when temperature gradients were established, and due to stray forward scattering from the multiple optical surfaces which are necessary when using cryogenics. The experiment on water was consequently repeated successfully, but under more "ideal" conditions, that is, using larger cell dimensions to make wall effects negligible. Water is a good candidate because of the relatively small  $\Gamma$ , but particularly because of the very small  $(\partial N/\partial T)_p$  relative to other liquids.  $N$  is the refractive index and the latter quantity determines how much the light beam bends and defocuses in the presence of a temperature gradient. This turns out to be a very important consideration since it was found to be impossible to pass a laser beam through the cell using other liquids under comparable temperature gradients. The disadvantages of water are that it is a poor light scatterer and that it is extremely difficult to eliminate dust, which scatters strongly at small angles.

The experiment was also successfully carried out on fused quartz at room temperature, and represents the first time that the Brillouin asymmetry induced by a temperature gradient has been observed in a solid.

The Brillouin spectrometer and geometry used in these experiments is shown schematically in Fig. 1. The incident light was provided by a single mode argon ion laser at a power level of about 100 mW. The scattered light was spatially filtered (SF) and analyzed at  $\alpha \sim 1^\circ$  with a piezoelectrically scanned confocal Fabry-Perot interferometer, of 1.00 GHz free spectral range, and detected by a cooled photomultiplier tube (PM). The output from the photomultiplier was coupled to a data acquisition and stabilization sys-

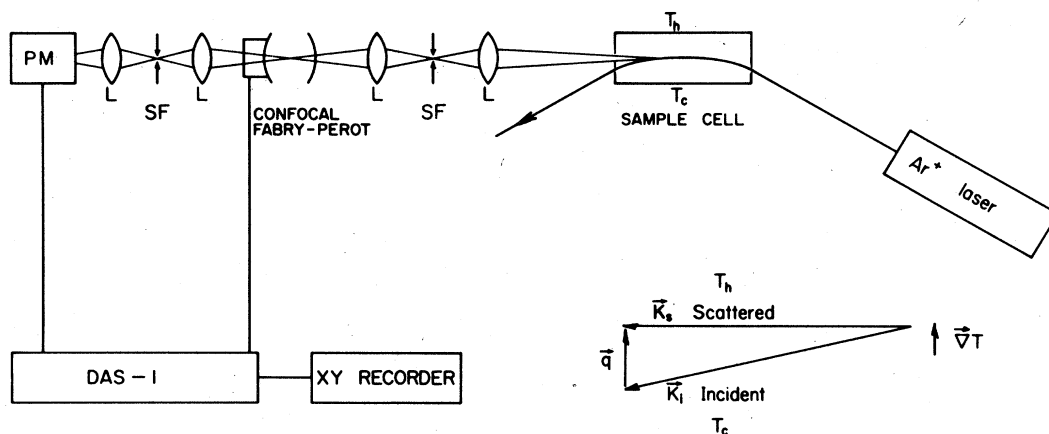


FIG. 1. Experimental setup and geometry.  $T_h$  and  $T_c$  are hot and cold sides of the sample, i.e.,  $\Delta T = T_h - T_c$ .

tem (Burleigh DAS-1). The multichannel analyzer of the DAS accumulated spectral data in the form of photon counts (intensity) versus channel number (proportional to the frequency of the scattered light). The resolution of this system was about 15 MHz.

The deionized water sample was carefully filtered numerous times through 0.2- $\mu\text{m}$  Teflon filters and contained in a  $1.0 \times 1.0 \times 4.0 \text{ cm}^3$  Spectrosil spectrophotometer cell. A fused quartz window was epoxied on the end so that the laser beam passes through lengthwise (see Fig. 1) and the gradient was applied via electrically heated and liquid- $\text{N}_2$ -cooled brass blocks across the 1.0-cm width of the cell (almost perpendicular to the incident laser beam). In this way a temperature gradient of up to  $45 \text{ K cm}^{-1}$  was obtained, and was measured directly by a copper-Constantan thermocouple mounted inside the cell. The gradient was always maintained vertically upwards for fluid stability.

About 100 spectra (and data points) were taken, examples of which are shown in Fig. 2. Dust in the water presented the major difficulty. Even after tedious filtering procedures, it was necessary to let the samples sit for about a month before being used. Because every few hours a tiny particle would cross the beam and spoil the data, it was necessary to use a series of many short ( $\sim 1 \text{ h}$ ) accumulation times.

The  $\vec{q}$  vector is determined from measured Brillouin frequency shifts in the observed spectra, using the relation  $\nu_s = \nabla \cdot \vec{q}$ . The velocity data tabulated by Rouch, Lai, and

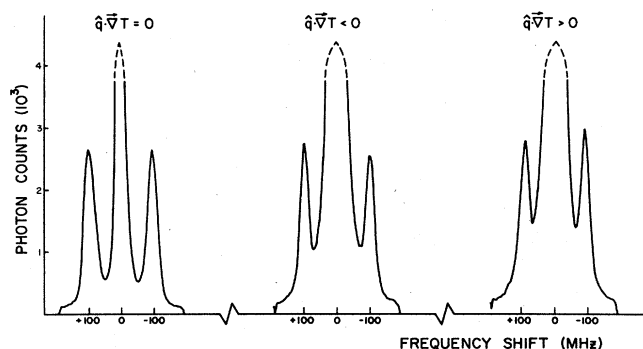


FIG. 2. Experimental spectra for water, examples at 4050, 4130, and  $3580 \text{ cm}^{-1}$ , respectively,  $\nabla T = 45 \text{ K cm}^{-1}$  and  $T = 307 \text{ K}$ .

Chen<sup>16</sup> were used. The  $\vec{q}$  vectors (in water) ranged from about  $2000\text{--}7000 \text{ cm}^{-1}$ ,  $\nabla T$  from  $0\text{--}45 \text{ K cm}^{-1}$ , and  $T$  from  $288\text{--}307 \text{ K}$ . The experimental asymmetry has been plotted as a function of  $\hat{q} \cdot \nabla T / q^2$  as shown in Figs. 3(a) and 3(b). Due to overlap of points, not all data is shown. The largest uncertainty in the data is in the determination of  $\epsilon$ ; it is estimated to be about 20%, but it is random in nature. That data of Fig. 3(b) are considered to be the "best."

Similar experiments were carried out on a block of high-quality fused quartz  $1.0 \times 1.0 \times 5.0 \text{ cm}^3$ . The Brillouin scattering was very weak and spectra were usually accumulated overnight. The  $\vec{q}$  vectors ranged from about  $4000\text{--}8000 \text{ cm}^{-1}$ ,  $\nabla T$  was estimated (with  $\sim 20\%$  uncertainty) to be about  $80 \text{ K cm}^{-1}$ , and  $T$  was about  $315 \text{ K}$ . The data are plotted in Fig. 3(c).

The following points need to be carefully considered in analyzing the data: the sound velocity variation in the scattering volume, the influence of the finite aperture angle, the finite beam diameter, and the defocusing effects due to the gradient. Some of the above have been considered by the theorists<sup>9</sup> and, as discussed by Beysens,<sup>15</sup> these effects are negligible. The conditions in the present experiment are more "ideal" than those of Beysens and should allow for better comparison with linear theory. Simple linear theory requires that the ratios (i)  $\Delta T/T$ , (ii)  $l_H/L$ , and (iii)  $l_H/L_{\nabla}$  all be much less than unity<sup>2</sup> (see also Refs. 3, 8, and 9), where  $L$  is the size of the system,  $l_H$  the hydrodynamic attenuation length or mean free path of the sound waves,  $L_{\nabla} = (|\nabla \ln T|)^{-1}$ , and  $\Delta T = L |\nabla T|$ . Condition (i), to leading order in  $\Delta T/T$ , allows for neglect of the temperature dependence of the transport coefficients and thermodynamic derivatives in the determination of the steady state. Condition (ii) allows for neglect of finite-size effects or boundary conditions. Condition (iii) characterizes and allows for neglect of nonlinearities. In the present work  $\Delta T/T \sim 0.15$ ,  $l_H/L = 0.15\text{--}3$ , and  $l_H/L_{\nabla} \sim 0.02\text{--}0.4$  (most data being at the lower ends) versus Beysens'  $\sim 0.16$ ,  $\sim 3\text{--}6$ , and  $\sim 0.5\text{--}1$ , respectively.<sup>2,15</sup>

From Figs. 3(a) and 3(b) there is clearly a region where the linear dependence of  $\epsilon_{\text{expt}}$  with  $\hat{q} \cdot \nabla T / q^2$  is well verified, for water. The experiment slopes are  $1.2 \times 10^4 \text{ K}^{-1} \text{ cm}^{-1}$  [Fig. 3(a)] and  $2.3 \times 10^4 \text{ K}^{-1} \text{ cm}^{-1}$  [Fig. 3(b)]. The theoretically expected slope is  $\nu/2\Gamma T$  and comparison with experiment depends on available  $\Gamma$  data. Rouch, Lai,

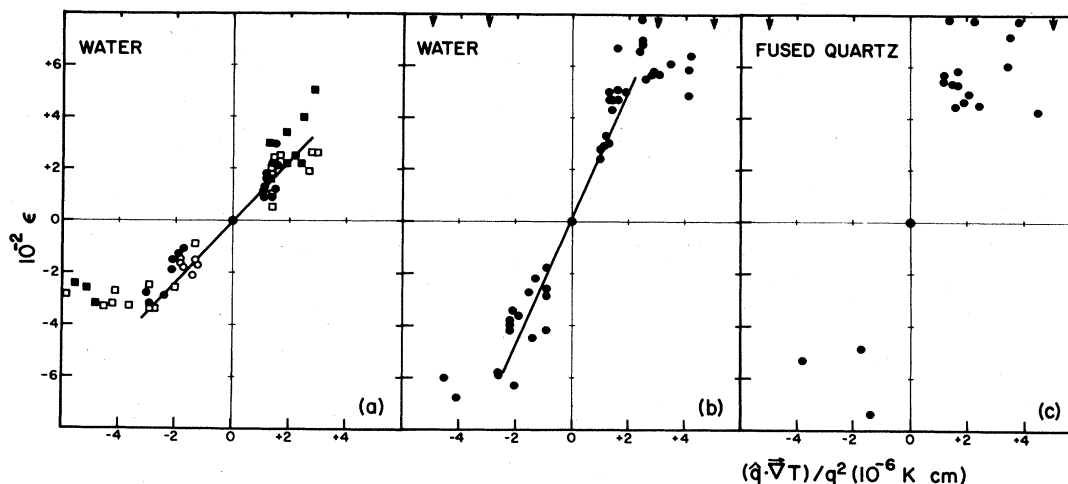


FIG. 3. Intensity asymmetry  $\epsilon$  vs  $\hat{q} \cdot \nabla T/q^2$ . (a) Mixture of data for water with  $\nabla T = 17$ – $40 \text{ K cm}^{-1}$  and  $T = 288 \text{ K}$  (open circles),  $293 \text{ K}$  (closed circles),  $298 \text{ K}$  (open squares), and  $303 \text{ K}$  (closed squares).  $\langle \nabla T \rangle = 28.3 \text{ K cm}^{-1}$  and  $\langle T \rangle = 296 \text{ K}$ . (b) "Best" data for water with  $\nabla T = 45 \text{ K cm}^{-1}$  and  $T = 307 \text{ K}$ . Outer arrows at top represent  $3000 \text{ cm}^{-1}$ , inner arrows  $4000 \text{ cm}^{-1}$ . (c) Data for fused quartz with  $\nabla T \sim 80 \text{ K cm}^{-1}$  and  $T \sim 315 \text{ K}$ . Arrows at top represent  $4000 \text{ cm}^{-1}$ . There appear to be oscillations in the data at  $+\epsilon$ .

and Chen<sup>16</sup> tabulate two curves  $\Gamma$  vs  $T$ . The higher valued  $\Gamma$  (based on work by David and Litovitz,<sup>17</sup> and Low<sup>18</sup>) was apparently used by Beysens.<sup>15</sup> Using this data for Fig. 3(a) gives  $1.3 \times 10^4 \text{ K}^{-1} \text{ cm}^{-1}$  and for Fig. 3(b)  $1.9 \times 10^4 \text{ K}^{-1} \text{ cm}^{-1}$ . Using the lower valued  $\Gamma$  (based on work by Rouch, Lai, and Chen, and Breitschwerdt and Kistenmacher<sup>19</sup>) for Fig. 3(a) gives  $1.9 \times 10^4 \text{ K}^{-1} \text{ cm}^{-1}$  and for Fig. 3(b)  $2.5 \times 10^4 \text{ K}^{-1} \text{ cm}^{-1}$ . Considering the uncertainty in  $\Gamma$  data and the present measurements, this represents excellent agreement.

It is also evident that the behavior is no longer linear for  $q < 3000$ – $4000 \text{ cm}^{-1}$  [see Fig. 3(b) in particular]. This is almost certainly due to finite-size effects<sup>14</sup> although nonlinear or mode-coupling effects<sup>9</sup> cannot be excluded. Satten and Ronis<sup>14</sup> discuss the interaction with sample surfaces. The dependence on surface reflection was much weaker than expected. A plot of  $\log \epsilon$  vs  $\log q$  (for the acoustic reflection coefficient  $R = \frac{1}{3}$ ,  $\nabla T = 59 \text{ K cm}^{-1}$ , and  $T = 313 \text{ K}$ )<sup>14</sup> shows the curve for  $L = 1.03 \text{ cm}$  break away from  $L = \infty$  for  $q \leq 3000$ – $4000 \text{ cm}^{-1}$ , and become constant at a value of  $\epsilon \approx 0.07$ . Despite slightly different conditions, this compares very nicely with a maximum  $\epsilon \sim 0.06$  in the present work. It is clear that the sample surfaces quench the long-range correlations and that Satten and Ronis calculations are consistent with the present experiments.

In the paper of Kirkpatrick, Cohen, and Dorfman<sup>9</sup> a plot of  $\epsilon$  vs  $\hat{q} \cdot \nabla T/q^2$  illustrates the nonlinear effects of mode coupling in large gradients. The net effect on  $\epsilon$  is somewhat similar to, and consequently difficult to clearly distinguish from, that due to finite-size effects. Such a distinction could be made by a study of the shape and intensity of the Rayleigh line since it shows deviations from equilibrium

which are proportional to  $(\nabla T)^2$ . Experimentally, however, that is not feasible. The issue could, in principle, also be resolved by checking whether or not the asymmetry is proportional to  $\nabla T$  in the region where the results deviate from a straight line. The present data do not allow this. However, in the present work the parameter  $l_H/L_\nabla$  is almost an order of magnitude smaller than  $l_H/L$ . It is, therefore, expected that the effects of boundaries should be greater as, indeed, appears to be the case on comparison with calculations of Satten and Ronis.<sup>14</sup> A theory that takes into account both wall effects and large gradients is necessary.

The data for fused quartz are preliminary, and from Fig. 3(c) it is evident that the effect is qualitatively the same; it has not previously been observed in a solid. A discussion by Fabelinskii,<sup>4</sup> based on earlier work, predicts an intensity asymmetry in solids which is proportional to  $\nabla T$ ,  $1/T$ , and  $1/\alpha = 1/\Gamma q^2$ . The geometry is not correct and the treatment is rough in that calculations are based on a phenomenological equation which expresses the balance between absorption and thermal generation. He assumes that the hydrodynamic limit is good up to  $90^\circ$  scattering and, hence, predicts huge effects in quartz and sapphire at low temperatures. Later, Griffin<sup>5</sup> considered this problem more microscopically and concluded that in the kinetic limit, the asymmetry is determined by umklapp scattering and, therefore, would not show up in the hydrodynamic regime. Further theoretical work on solids is necessary before more meaningful experimental comparisons can be made.

The authors acknowledge with pleasure the helpful and valuable discussions with Dr. A.-M. S. Tremblay.

<sup>1</sup>See, entire issue of Phys. Today 37 (No. 1) (1984).

<sup>2</sup>A.-M. S. Tremblay, in *Recent Developments in Nonequilibrium Thermodynamics*, Lecture Notes in Physics, Vol. 199, edited by J. Casas-Vazques and D. Jou (Springer-Verlag, Berlin, 1984).

<sup>3</sup>A.-M. S. Tremblay, M. Arai, and E. D. Siggia, Phys. Rev. A 23, 1451 (1981).

<sup>4</sup>I. L. Fabelinskii, *Molecular Scattering of Light* (Plenum, New York, 1968).

- <sup>5</sup>A. Griffin, *Can. J. Phys.* **46**, 2843 (1968).
- <sup>6</sup>I. Procaccia, D. Ronis, and I. Oppenheim, *Phys. Rev. Lett.* **42**, 287 (1979); *Phys. Rev. A* **20**, 2533 (1979).
- <sup>7</sup>D. Ronis, I. Procaccia, and I. Oppenheim, *Phys. Rev. A* **19**, 1290 (1979); **19**, 1307 (1979); **19**, 1324 (1979).
- <sup>8</sup>T. Kirkpatrick, E. G. D. Cohen, and J. R. Dorfman, *Phys. Rev. Lett.* **42**, 862 (1979); **44**, 472 (1980).
- <sup>9</sup>T. R. Kirkpatrick, E. G. D. Cohen, and J. R. Dorfman, *Phys. Rev. A* **26**, 950 (1982); **26**, 972 (1982); **26**, 995 (1982).
- <sup>10</sup>A.-M. S. Tremblay, E. D. Siggia, and M. R. Arai, *Phys. Lett.* **76A**, 57 (1980).
- <sup>11</sup>C. Tremblay and A.-M. S. Tremblay, *Phys. Rev. A* **25**, 1962 (1982).
- <sup>12</sup>G. van der Zwan and P. Mazur, *Phys. Lett.* **75A**, 370 (1980); *Physica A* **107**, 491 (1981).
- <sup>13</sup>D. Ronis, I. Procaccia, and J. Machta, *Phys. Rev. A* **22**, 714 (1980).
- <sup>14</sup>G. Satten and D. Ronis, *Phys. Rev. A* **26**, 940 (1982).
- <sup>15</sup>D. Beysens, Y. Garrabos, and G. Zalczer, *Phys. Rev. Lett.* **45**, 403 (1980).
- <sup>16</sup>J. Rouch, C. C. Lai, and S. H. Chen, *J. Chem. Phys.* **65**, 4016 (1976).
- <sup>17</sup>C. M. David and T. A. Litovitz, *J. Chem. Phys.* **42**, 2563 (1965).
- <sup>18</sup>M. Low, *J. Phys. (Paris) Colloq.* **33**, C1-1 (1972).
- <sup>19</sup>K. G. Breitschwerdt and H. Kistenmacker, *J. Chem. Phys.* **56**, 4800 (1972).